Supplementary Information

Chemical bonding in electron-deficient boron oxide clusters: core boronyl group, dual 3c-4e hypervalent bond, and rhombic 4c-4e bond†

Qiang Chen, Haigang Lu, Hua-Jin Zhai,* and Si-Dian Li*

Nanocluster Laboratory, Institute of Molecular Science, Shanxi University, Taiyuan 030006, China

E-mail: hj.zhai@sxu.edu.cn; lisidian@sxu.edu.cn

Full citation of ref 22.

Tables S1–S7 Natural charges, natural resonance theory (NRT) bond orders and atomic valencies for the global-minimum structures **3–9** of $B_3O_2^+$, $B_3O_3^{-/0/+}$, and $B_3O_4^{-/0/+}$.

Table S8 Calculated vertical electron detachment energies (VDEs) at the TD-B3LYP level based on the global minimum structures $D_{\infty h}$ $B_3O_2^-$ (**1**, $^3\Sigma_g$), C_{2v} $B_3O_3^-$ (**4**, $^1A_1$), and C_{2v} $B_3O_4^-$ (**7**, $^1A_1$).

Figs. S1–S7 Alternative optimized structures for $B_3O_2^+$, $B_3O_3^{-/0/+}$, and $B_3O_4^{-/0/+}$, along with their point group symmetries, electronic states, and minimum vibrational frequencies. Relative energies are given at B3LYP/aug-cc-pVTZ and CCSD(T)//B3LYP/aug-cc-pVTZ (in curly brackets). The structures were obtained initially using the Coalescence Kick and Basin Hopping global-minimum search programs at B3LYP/3-21G.

Figs. S8–S15 AdNDP bonding patterns and canonical molecular orbitals (CMOs) for the global-minimum structures **3–9** of $B_3O_2^+$, $B_3O_3^{-/0/+}$, and $B_3O_4^{-/0/+}$. A low-lying $D_{\infty h}$ $B_3O_2^+$ ($^1\Sigma_g$) structure is also analyzed.

Full citation of ref 22.

22 Gaussian 09, Revision A.2, M. J. Frisch, G. W. Trucks, H. B. Schlegel, G. E. Scuseria, M. A. Robb, J. R. Cheeseman, G. Scalmani, V. Barone, B. Mennucci, G. A. Petersson, H. Nakatsuji, M. Caricato, X. Li, H. P. Hratchian, A. F. Izmaylov, J. Bloino, G. Zheng, J. L. Sonnenberg, M. Hada, M. Ehara, K. Toyota, R. Fukuda, J. Hasegawa, M. Ishida, T. Nakajima, Y. Honda, O. Kitao, H. Nakai, T. Vreven, J. A. Montgomery, Jr., J. E. Peralta, F. Ogliaro, M. Bearpark, J. J. Heyd, E. Brothers, K. N. Kudin, V. N. Staroverov, R. Kobayashi, J. Normand, K. Raghavachari, A. Rendell, J. C. Burant, S. S. Iyengar, J. Tomasi, M. Cossi, N. Rega, J. M. Millam, M. Klene, J. E. Knox, J. B. Cross, V. Bakken, C. Adamo, J. Jaramillo, R. Gomperts, R. E. Stratmann, O. Yazyev, A. J. Austin, R. Cammi, C. Pomelli, J. W. Ochterski, R. L. Martin, K. Morokuma, V. G. Zakrzewski, G. A. Voth, P. Salvador, J. J. Dannenberg, S. Dapprich, A. D. Daniels, Ö. Farkas, J. B. Foresman, J. V. Ortiz, J. Cioslowski, and D. J. Fox, Gaussian, Inc., Wallingford CT, 2009.

Table S1. Natural resonance theory (NRT) bond orders and atomic valencies of $C_{\infty v}$ $B_3O_2^+$ (**3**, $^1\Sigma$) at B3LYP/aug-cc- pVTZ. The bond lengths (in Å) and natural atomic charges (in |e|) are also labeled.

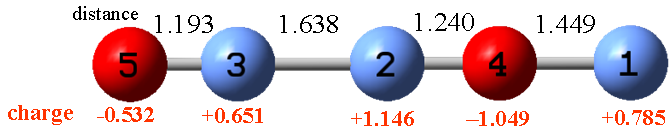

$C_{\infty v}$ $B_3O_2^+$ ($^1\Sigma$)

		Natural Bond Order				Natural Atomic Valency				
		B_1-O_4	B_2-B_3	B_2-O_4	B_3-O_5	O_5	B_3	B_2	O_4	B_1
NRT	t[a]	1.03	1.03	2.93	2.97	2.97	3.99	3.95	3.97	1.03
	c	0.17	0.93	0.72	1.39	1.39	2.32	1.65	0.89	0.17
	i	0.86	0.10	2.21	1.58	1.58	1.67	2.30	3.08	0.86

[a] t, the total bond orders; c, the covalent bond orders of NRT; i, the ionic bond orders of NRT.

Table S2. Natural resonance theory (NRT) bond orders and atomic valencies of C_{2v} $B_3O_3^-$ (**4**, $^1A_1$) at B3LYP/aug-cc- pVTZ. The bond lengths (in Å) and natural atomic charges (in |e|) are also labeled.

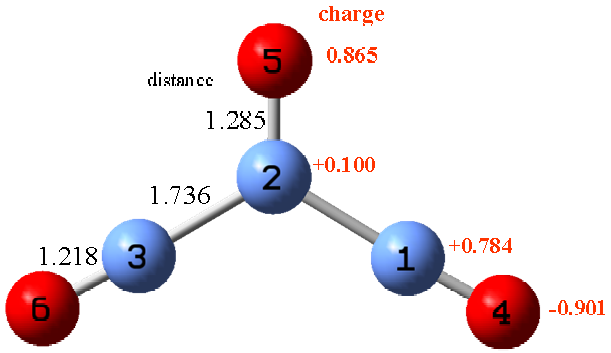

C_{2v} $B_3O_3^-$ ($^1A_1$)

		Natural Bond Order					Natural Atomic Valencies			
		B_1-B_2	B_2-B_3	B_1-O_4	B_2-O_5	O_3-O_6	O_6	B_3	B_2	O_5
NRT	t[a]	0.98	0.98	2.98	2.04	2.98	2.98	3.96	4.00	2.04
	c	0.90	0.90	1.08	0.95	1.08	1.08	1.98	2.75	0.95
	i	0.08	0.08	1.90	1.09	1.90	1.90	1.98	1.25	1.09

[a] t, the total bond orders; c, the covalent bond orders of NRT; i, the ionic bond orders of NRT.

Table S3. Natural resonance theory (NRT) bond orders and atomic valencies of C_{2v} B_3O_3 (**5**, $^2A_1$) at B3LYP/aug-cc- pVTZ. The bond lengths (in Å) and natural atomic charges (in |e|) are also labeled.

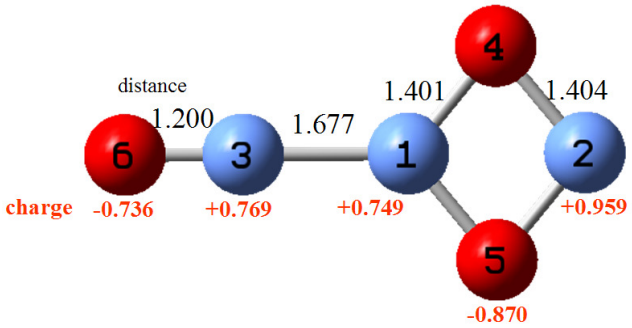

C_{2v} B_3O_3 ($^2A_1$)

		Natural Bond Order						Natural Atomic Valency					
		B_1-B_3	B_1-O_4	B_1-O_5	B_2-O_4	B_2-O_5	B_3-O_6	O_6	B_3	B_1	O_4	O_5	B_2
NRT[a]	t	0.99	1.45	1.45	1.46	1.46	3.00	3.00	3.98	3.88	2.91	2.91	2.92
	c	0.95	0.49	0.49	0.42	0.42	1.23	1.23	2.18	1.93	0.91	0.91	0.84
	i	0.04	0.96	0.96	1.04	1.04	1.77	1.77	1.80	1.95	2.00	2.00	2.08

[a] C_{2v} B_3O_3 ($^2A_1$) possesses two leading NRT reference structures: NRT_1 and NRT_2.

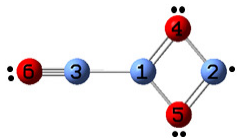

NRT_1 40%

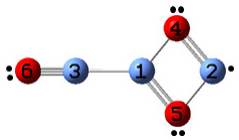

NRT_2 40%

Table S4. Natural resonance theory (NRT) bond orders and atomic valencies of $C_{\infty v}$ $B_3O_3^+$ (**6**, $^1\Sigma$) at B3LYP/aug-cc- pVTZ. The bond lengths (in Å) and natural atomic charges (in |e|) are also labeled.

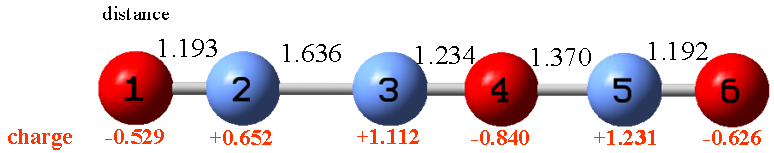

$C_{\infty v}$ $B_3O_3^+$ ($^1\Sigma$)

		Natural Bond Order					Natural Atomic Valencies					
		B_1-B_2	B_2-B_3	B_3-O_4	B_4-O_5	B_5-O_6	O_1	B_2	B_3	O_4	B_5	O_6
NRT	t[a]	2.97	1.02	2.91	1.04	2.95	2.97	3.99	3.93	3.95	4.00	2.95
	c	1.40	0.93	0.72	0.34	1.31	1.40	2.32	1.65	1.06	1.65	1.31
	i	1.57	0.09	2.19	0.70	1.64	1.57	1.67	2.28	2.89	2.35	1.64

[a] t, the total bond orders; c, the covalent bond orders of NRT; i, the ionic bond orders of NRT.

Table S5. Natural resonance theory (NRT) bond orders and atomic valencies of C_{2v} $B_3O_4^-$ (**7**, $^1A_1$) at B3LYP/aug-cc- pVTZ. The bond lengths (in Å) and natural atomic charges (in |e|) are also labeled in the structure.

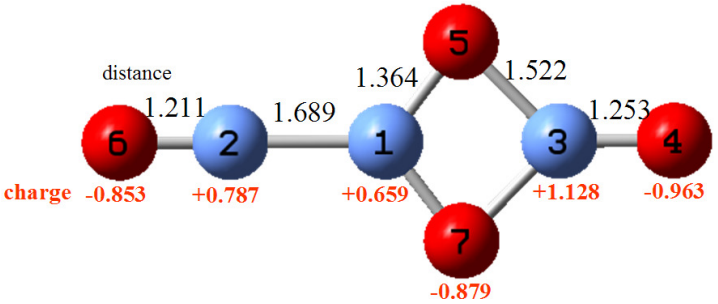

C_{2v} $B_3O_4^-$ ($^1A_1$)

		Natural Bond Order							Natural Atomic Valency						
		B_1-B_2	B_1-O_5	B_1-O_7	B_2-O_6	B_3-O_4	B_3-O_5	B_3-O_7	O_6	B_2	B_1	O_5	O_7	B_3	O_4
NRT[a]	t[b]	0.99	1.47	1.47	2.99	2.04	1.38	1.38	2.99	3.98	3.93	2.86	2.86	4.81	2.04
	c	0.95	0.53	0.53	1.13	0.82	0.34	0.34	1.13	2.08	2.01	0.88	0.88	1.51	0.82
	i	0.04	0.94	0.94	1.86	1.22	1.04	1.04	1.86	1.90	1.92	1.98	1.98	3.30	1.22

[a] C_{2v} $B_3O_4^-$ ($^1A_1$) possesses two significant NRT reference structures: NRT_1 and NRT_2.

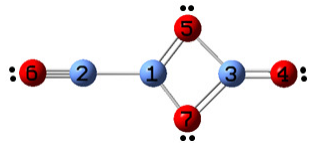

NRT_1 32%

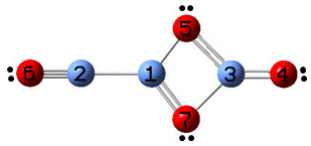

NRT_2 32%

[b] t, the total bond orders; c, the covalent bond orders of NRT; i, the ionic bond orders of NRT.

Table S6. Natural resonance theory (NRT) bond orders and atomic valencies of C_s B_3O_4 (**8**, $^2A'$) at B3LYP/aug-cc- pVTZ. The bond lengths (in Å) and natural atomic charges (in |e|) are also labeled.

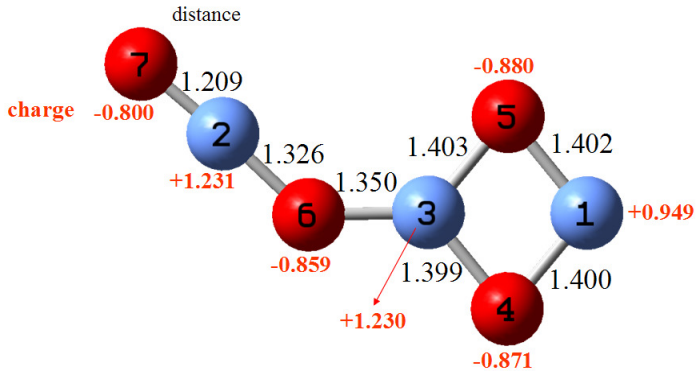

C_s B_3O_4 ($^2A'$)

		Natural Bond Order							Natural Atomic Valencies						
		B_1-O_4	B_1-O_5	B_2-O_6	B_2-O_7	B_3-O_4	B_3-O_5	B_3-O_6	O_7	B_2	O_6	B_3	O_4	O_5	B_1
NRT[a]	t	1.47	1.47	1.08	2.91	1.42	1.42	1.04	2.91	3.99	2.12	3.88	2.89	2.89	2.93
	c	0.43	0.43	0.39	1.16	0.48	0.48	0.40	1.16	1.56	0.79	1.36	0.91	0.90	0.85
	i	1.04	1.04	0.69	1.75	0.94	0.94	0.64	1.75	2.43	1.33	2.52	1.98	1.98	2.08

[a] C_s B_3O_4 ($^2A'$) possesses two leading NRT reference structures: NRT_1 and NRT_2.

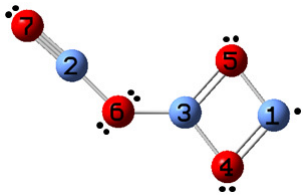

NRT_1 30%

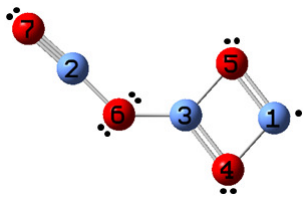

NRT_2 30%

Table S7. Natural resonance theory (NRT) bond orders and atomic valencies of $D_{\infty h}$ $B_3O_4^+$ (**9**, $^1\Sigma_g$) at B3LYP/aug-cc- pVTZ. The bond lengths (in Å) and natural atomic charges (in |e|) are also labeled.

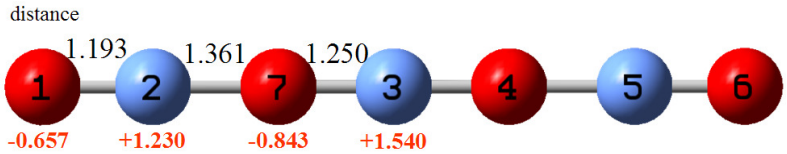

$D_{\infty h}$ $B_3O_4^+$ ($^1\Sigma_g$)

		Natural Bond Order					Natural Atomic Valencies				
		O_1-B_2	B_2-O_7	B_3-O_7	B_3-O_4	O_4-B_5	B_5-O_6	O_1	B_2	O_7	B_3
NRT[a]	T[b]	2.96	1.04	1.97	1.97	1.04	2.95	2.96	3.99	3.00	3.93
	c	1.30	0.34	0.55	0.55	0.34	1.30	1.30	1.64	0.89	1.10
	i	1.66	0.70	1.42	1.42	0.70	1.65	1.66	2.35	2.11	2.83

[a] $D_{\infty h}$ $B_3O_4^+$ ($^1\Sigma_g$) possesses three significant NRT reference structures: NRT_1, NRT_2 and NRT_3.

NRT_1 34%

NRT_2 34%

NRT_3 17%

[b] t, the total bond orders; c, the covalent bond orders of NRT; i, the ionic bond orders of NRT.

Table S8. Calculated vertical electron detachment energies (VDEs) at the TD-B3LYP level based on the global minimum structures $D_{\infty h}$ $B_3O_2^-$ (**1**, $^3\Sigma_g$), C_{2v} $B_3O_3^-$ (**4**, $^1A_1$), and C_{2v} $B_3O_4^-$ (**7**, $^1A_1$).

Species	Feature	Final State	VDE (eV)
$B_3O_2^-$ $D_{\infty h}$ (**1**, $^3\Sigma_g$)	X	$^2\Pi_u$	3.07
	A	$^2\Pi_u$	6.43
$B_3O_3^-$ C_{2v} (**4**, $^1A_1$)	X	$^2B_2$	4.06
	A	$^2B_2$	6.40
$B_3O_4^-$ C_{2v} (**7**, $^1A_1$)	X	$^2B_2$	5.10
	A	$^2A_2$	6.10

Figure S1. Alternative optimized structures for $B_3O_2^+$, along with their point group symmetries, electronic states, and minimum vibrational frequencies. Relative energies are given at B3LYP/aug-cc-pVTZ and CCSD(T)//B3LYP/aug-cc-pVTZ (in curly brackets). The structures were obtained initially using the Coalescence Kick and Basin Hopping global-minimum search programs at B3LYP/3-21G.

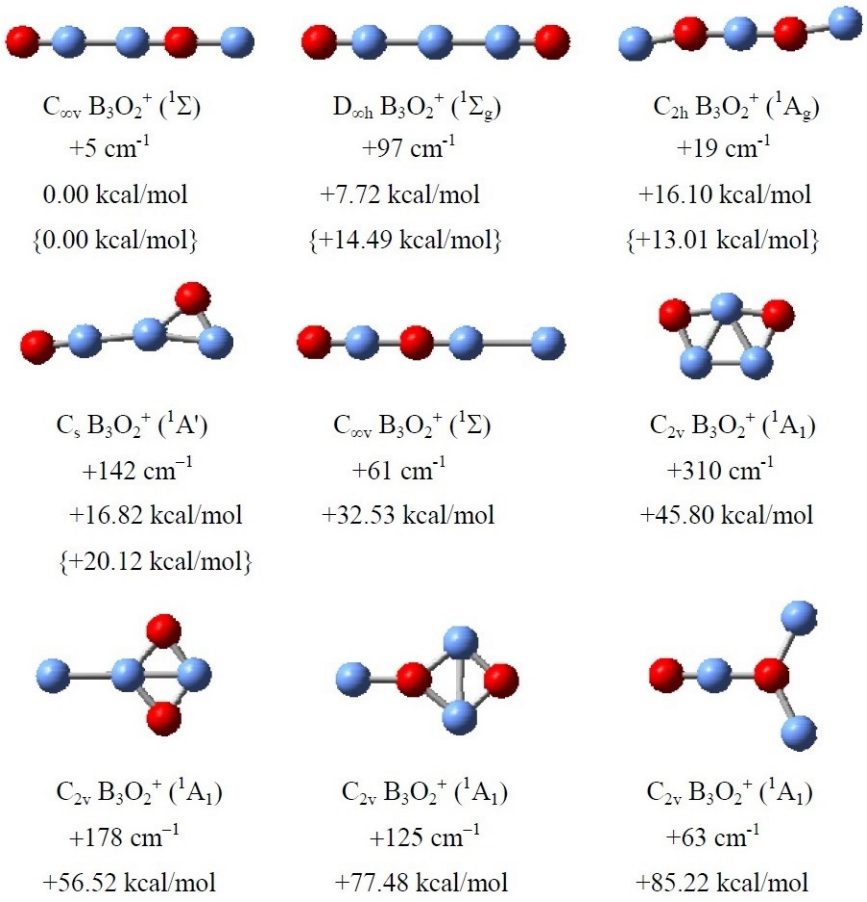

Figure S2. Alternative optimized structures for $B_3O_3^-$, along with their point group symmetries, electronic states, and minimum vibrational frequencies. Relative energies are given at B3LYP/aug-cc-pVTZ and CCSD(T)//B3LYP/aug-cc-pVTZ (in curly brackets). The structures were obtained initially using the Coalescence Kick and Basin Hopping global-minimum search programs at B3LYP/3-21G.

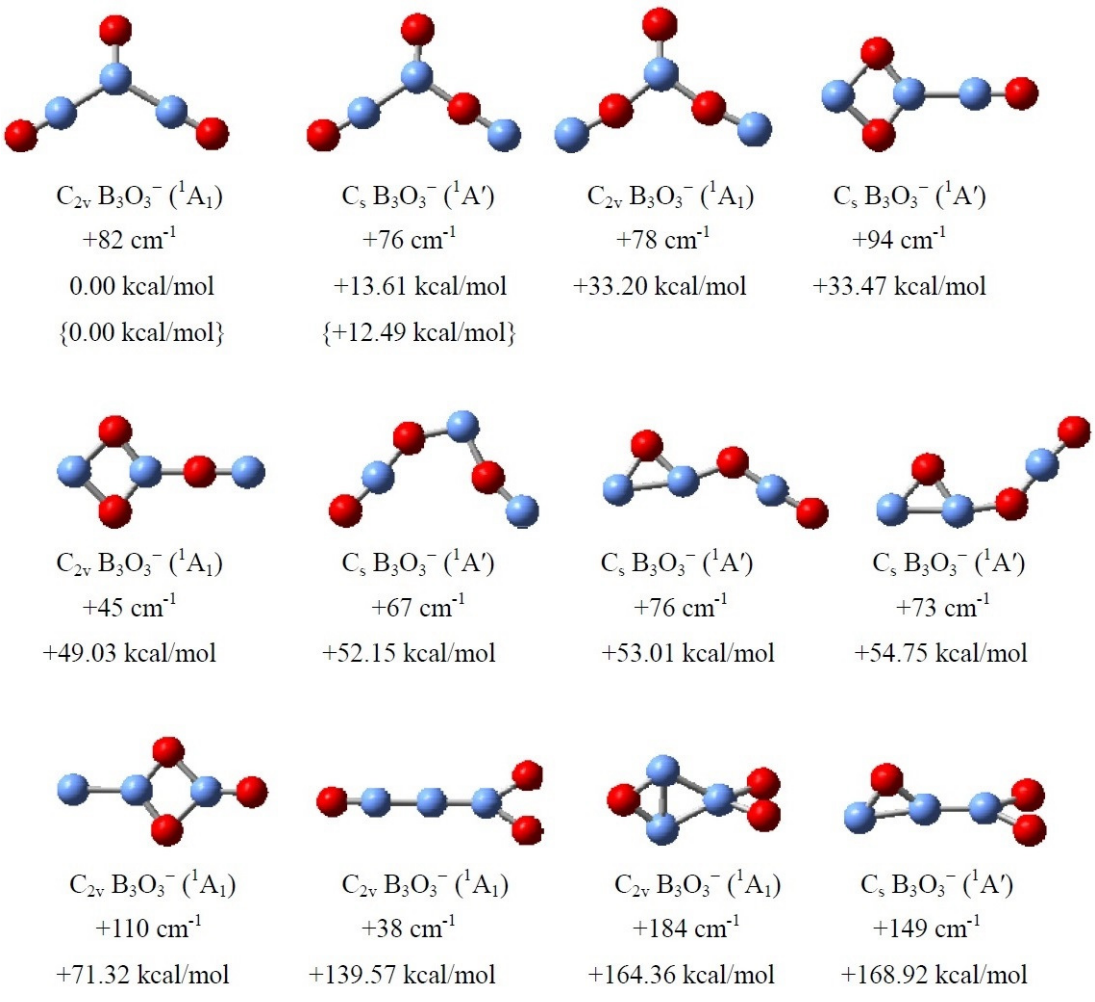

Figure S3. Alternative optimized structures for B_3O_3, along with their point group symmetries, electronic states, and minimum vibrational frequencies. Relative energies are given at B3LYP/aug-cc-pVTZ and CCSD(T)//B3LYP/aug-cc-pVTZ (in curly brackets). The structures were obtained initially using the Coalescence Kick and Basin Hopping global-minimum search programs at B3LYP/3-21G.

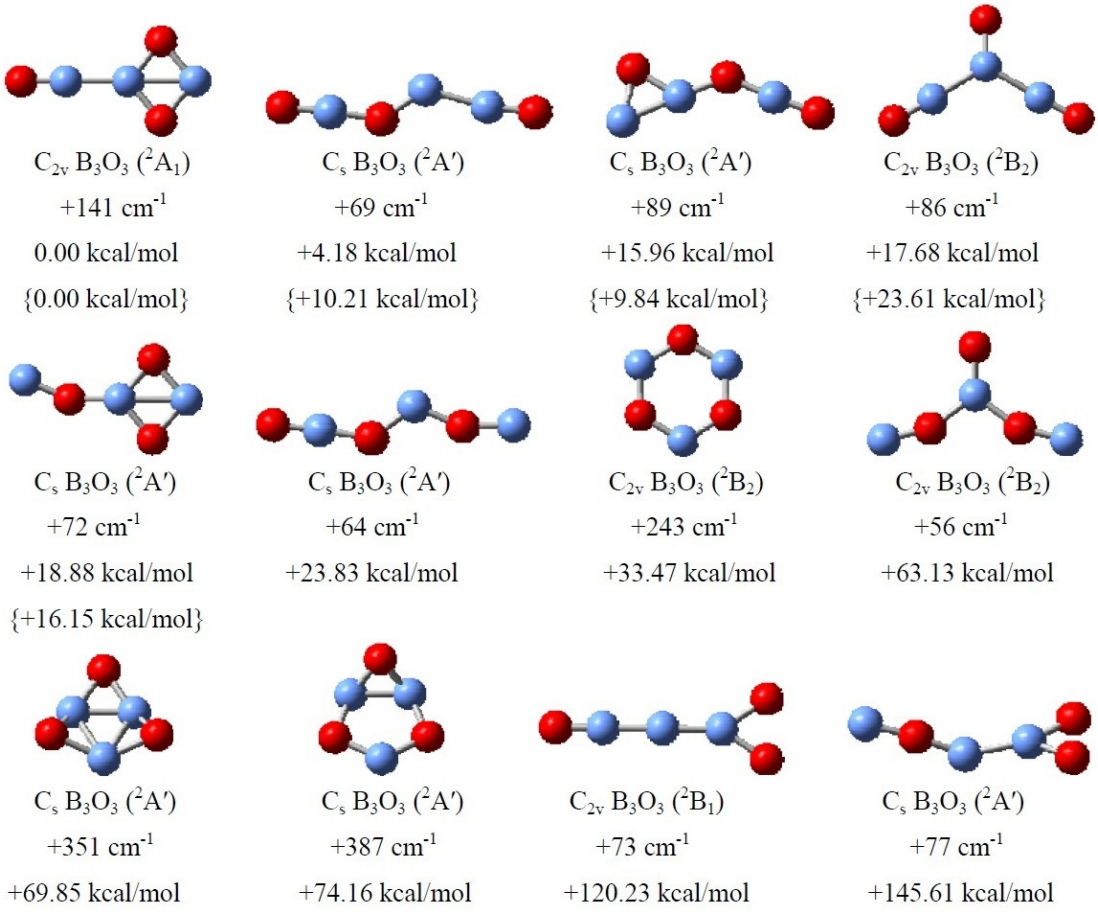

Figure S4. Alternative optimized structures for $B_3O_3^+$, along with their point group symmetries, electronic states, and minimum vibrational frequencies. Relative energies are given at B3LYP/aug-cc-pVTZ and CCSD(T)//B3LYP/aug-cc-pVTZ (in curly brackets). The structures were obtained initially using the Coalescence Kick and Basin Hopping global-minimum search programs at B3LYP/3-21G.

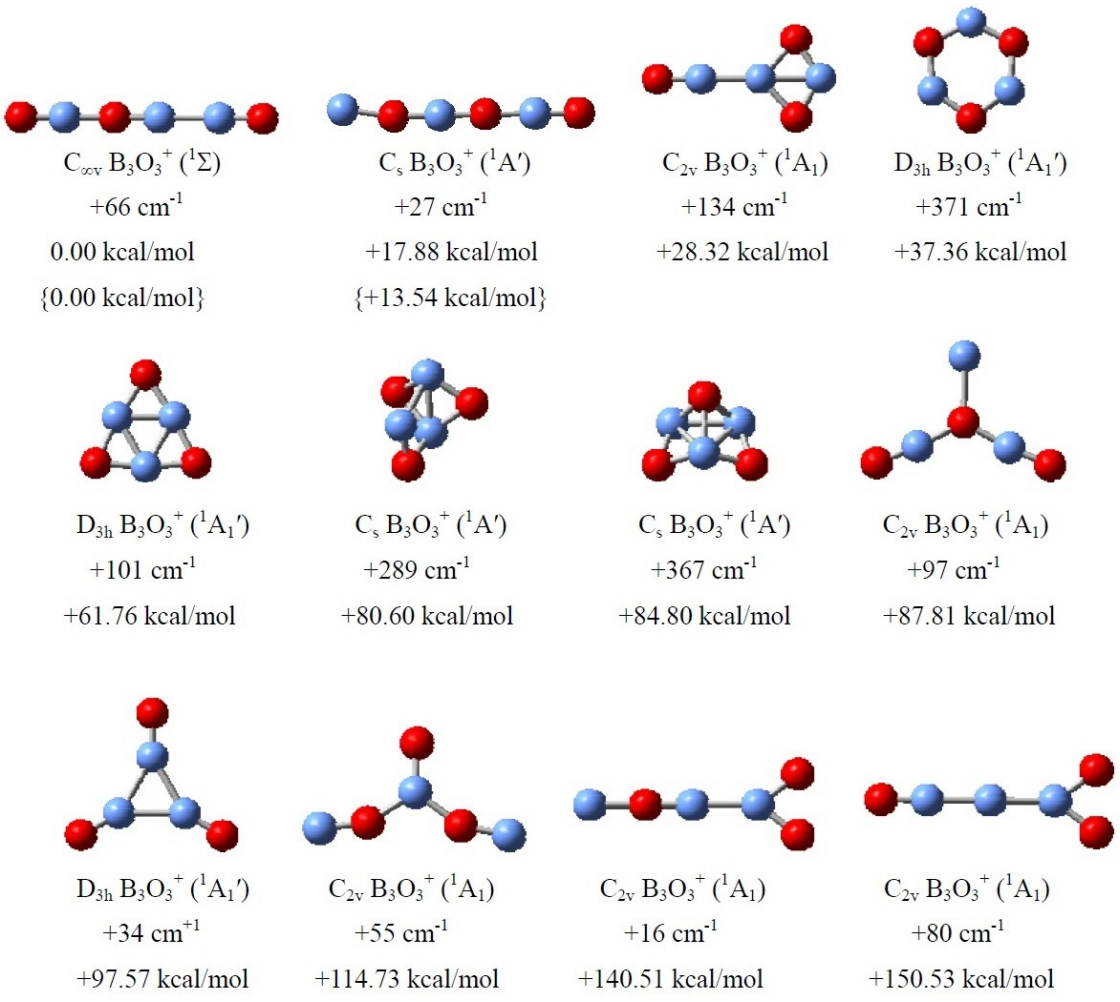

Figure S5. Alternative optimized structures for $B_3O_4^-$, along with their point group symmetries, electronic states, and minimum vibrational frequencies. Relative energies are given at B3LYP/aug-cc-pVTZ and CCSD(T)//B3LYP/aug-cc-pVTZ (in curly brackets). The structures were obtained initially using the Coalescence Kick and Basin Hopping global-minimum search programs at B3LYP/3-21G.

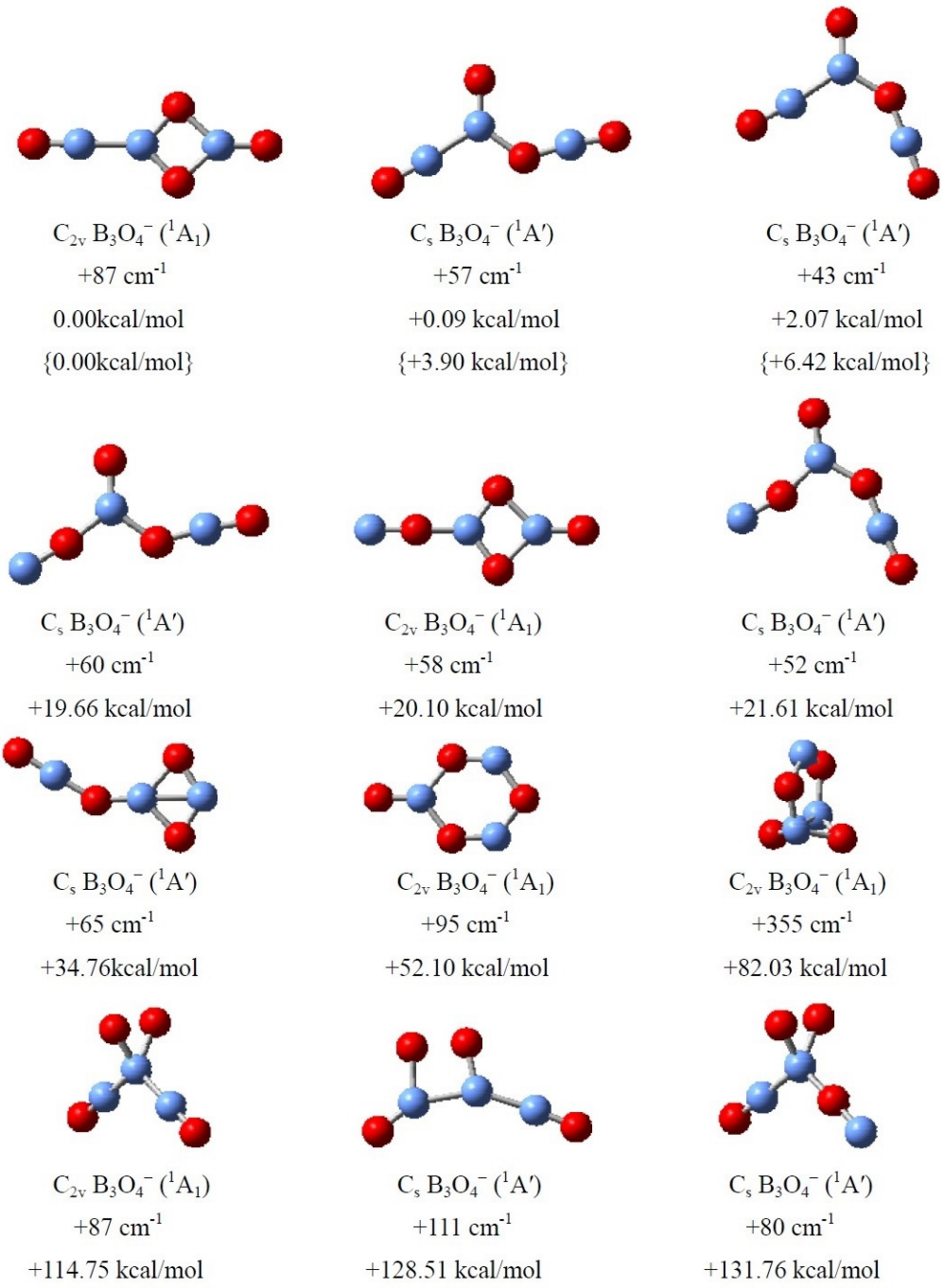

Figure S6. Alternative optimized structures for B_3O_4, along with their point group symmetries, electronic states, and minimum vibrational frequencies. Relative energies are given at B3LYP/aug-cc-pVTZ and CCSD(T)//B3LYP/aug-cc-pVTZ (in curly brackets). The structures were obtained initially using the Coalescence Kick and Basin Hopping global-minimum search programs at B3LYP/3-21G.

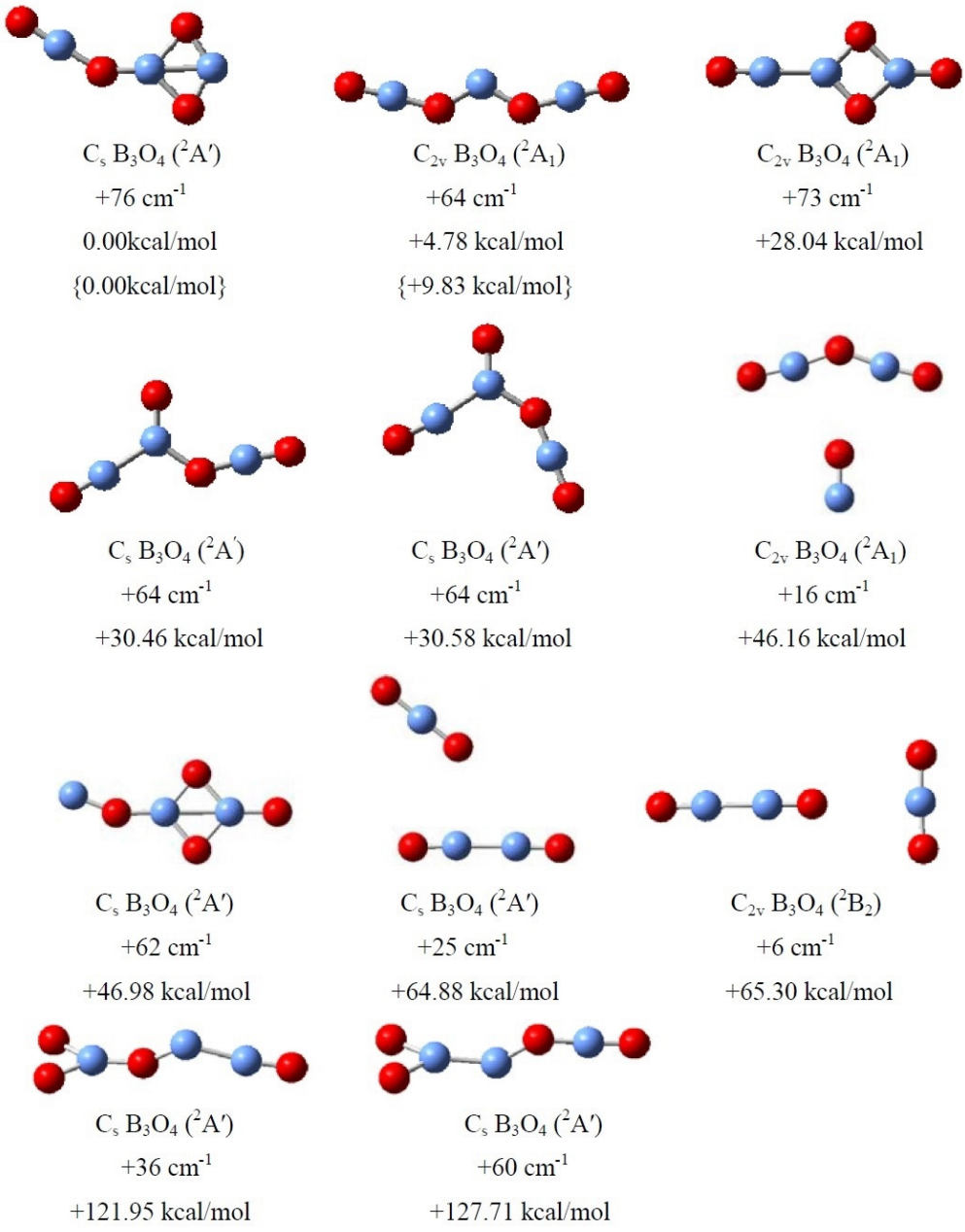

Figure S7. Alternative optimized structures for $B_3O_4^+$, along with their point group symmetries, electronic states, and minimum vibrational frequencies. Relative energies are given at B3LYP/aug-cc-pVTZ and CCSD(T)//B3LYP/aug-cc-pVTZ (in curly brackets). The structures were obtained initially using the Coalescence Kick and Basin Hopping global-minimum search programs at B3LYP/3-21G.

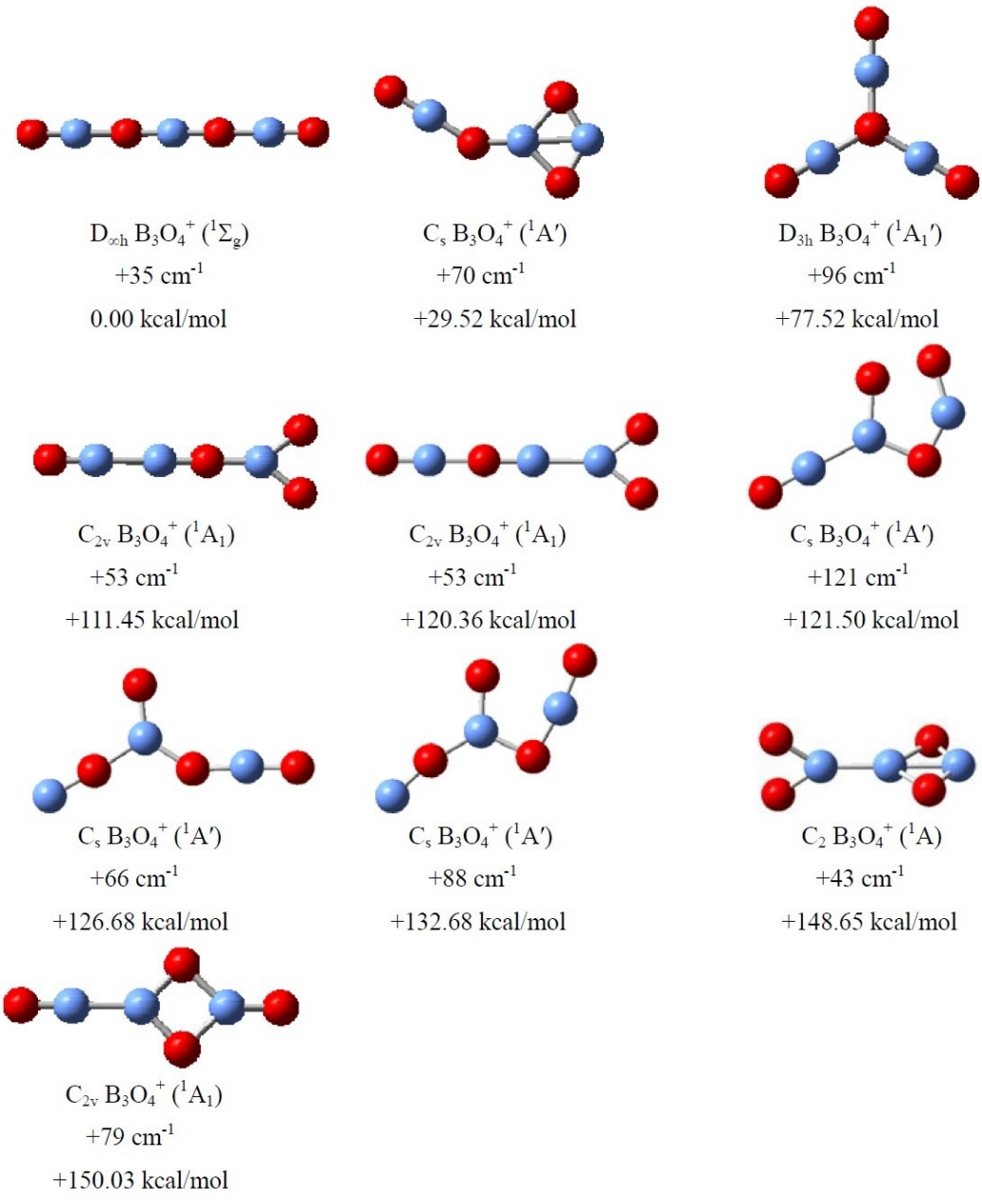

Figure S8. (a) AdNDP bonding pattern for the $C_{\infty v}$ $B_3O_2^+$ (**3**, $^1\Sigma$) global-minimum structure and (b) its canonical molecular orbitals (CMOs).

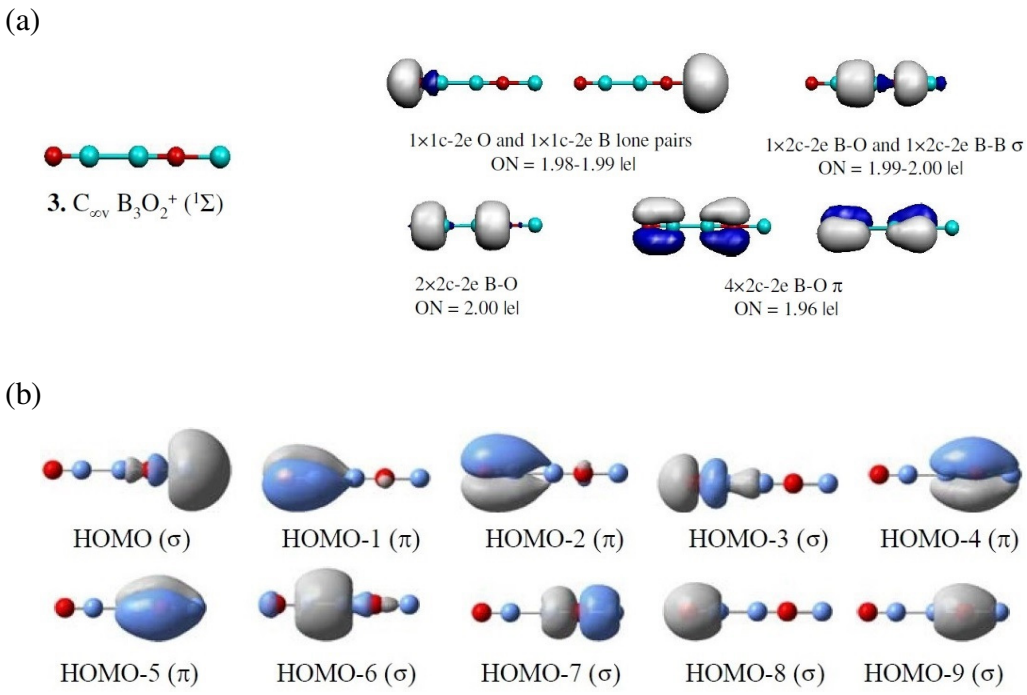

Figure S9. (a) AdNDP bonding pattern for $D_{\infty h}$ $B_3O_2^+$ ($^1\Sigma_g$) and (b) its canonical molecular orbitals (CMOs).

(a)

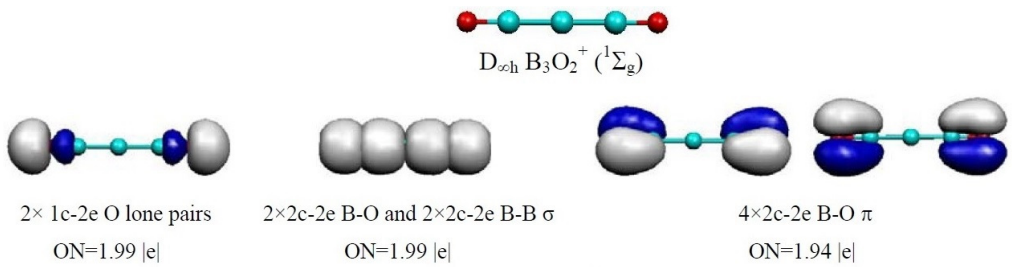

(b)

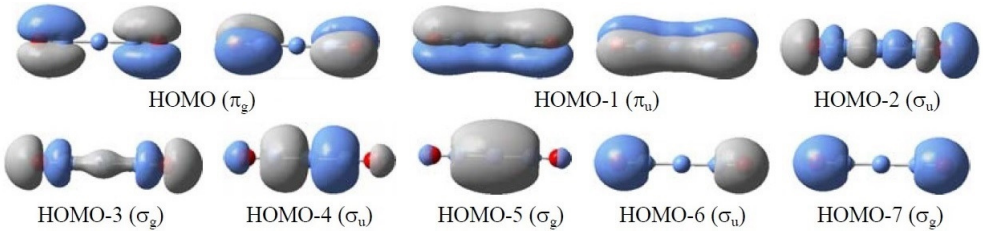

Figure S10. (a) AdNDP bonding pattern for the C_{2v} $B_3O_3^-$ (**4**, $^1A_1$) global-minimum structure and (b) its canonical molecular orbitals (CMOs).

(a)

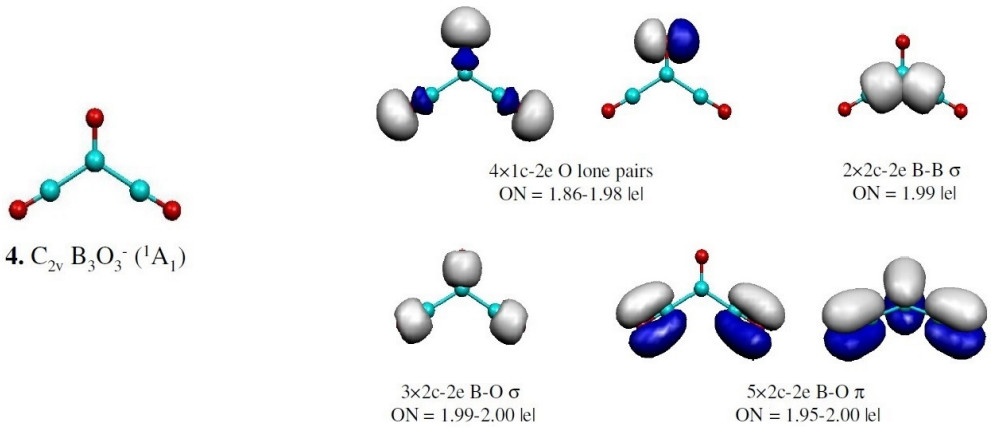

(b)

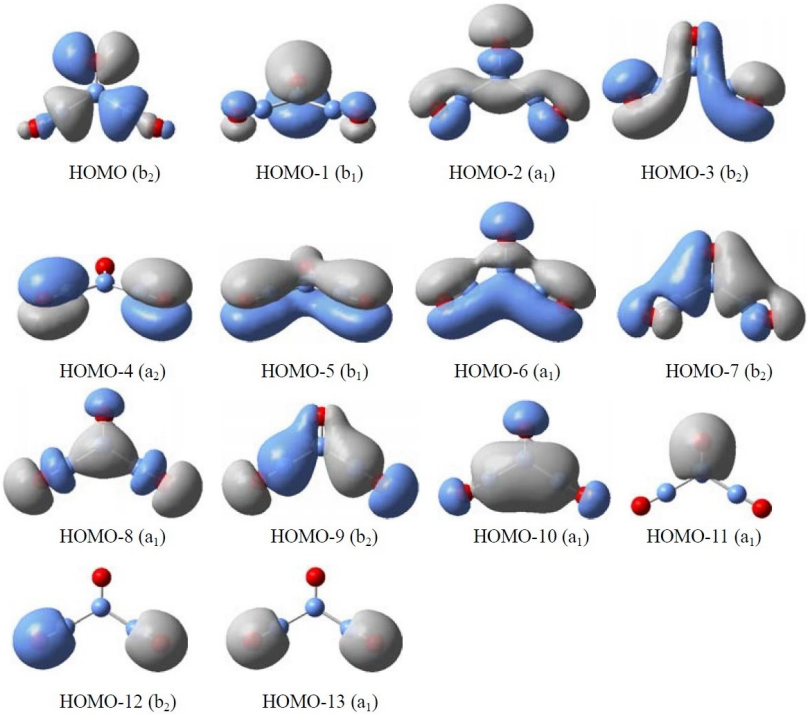

Figure S11. (a) AdNDP bonding pattern for the C_{2v} B_3O_3 (**5**, $^2A_1$) global-minimum structure and (b) its canonical molecular orbitals (CMOs).

(a)

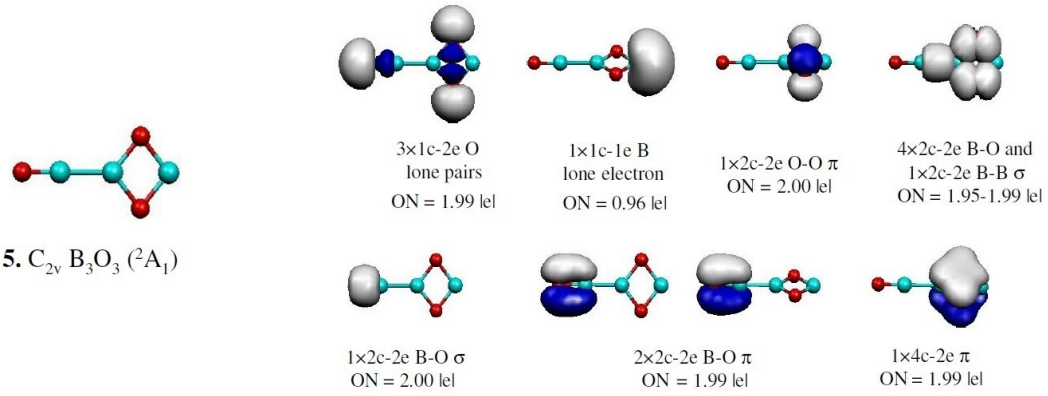

5. C_{2v} B_3O_3 ($^2A_1$)

(b)

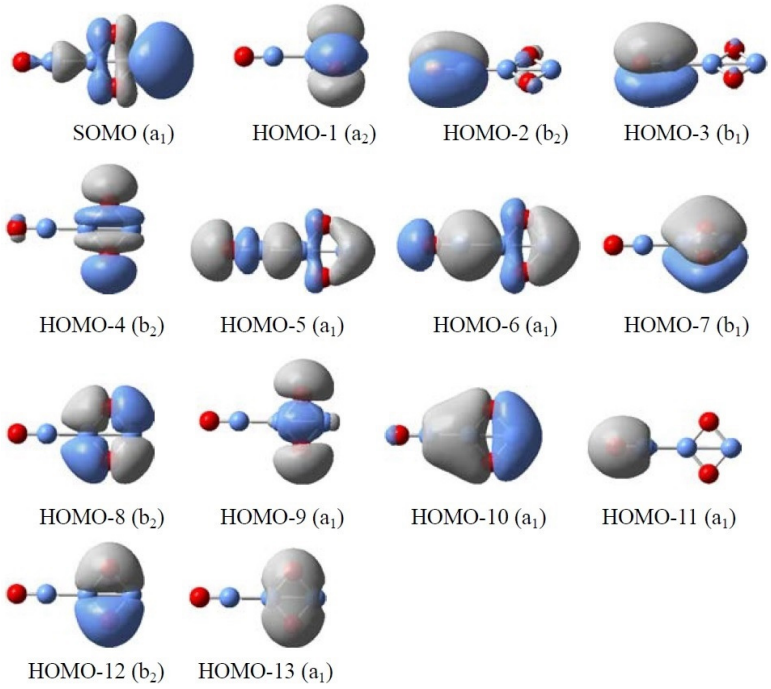

Figure S12. (a) AdNDP bonding pattern for the $C_{\infty v}$ $B_3O_3^+$ (**6**, $^1\Sigma$) global-minimum structure and (b) its canonical molecular orbitals (CMOs).

(a)

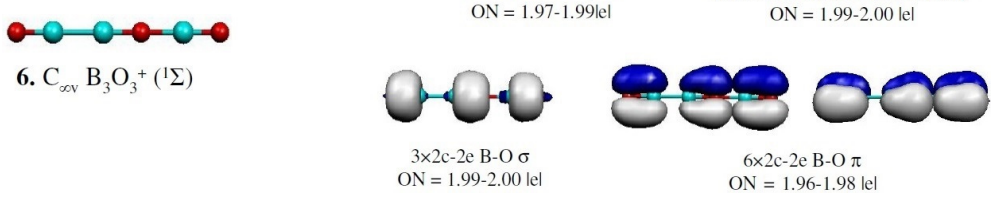

(b)

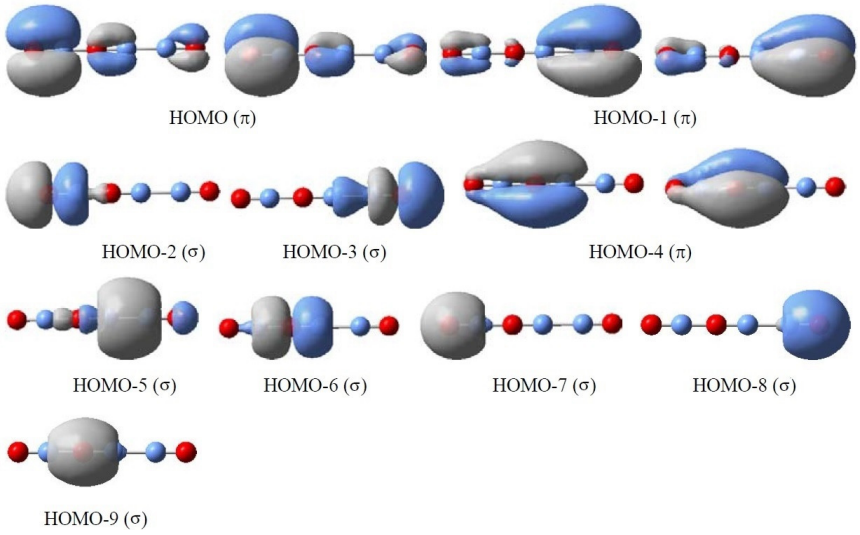

Figure S13. Canonical molecular orbitals (CMOs) for the C_{2v} $B_3O_4^-$ (**7**, $^1A_1$) global-minimum structure. For its AdNDP bonding pattern, see Figure 4 in the text.

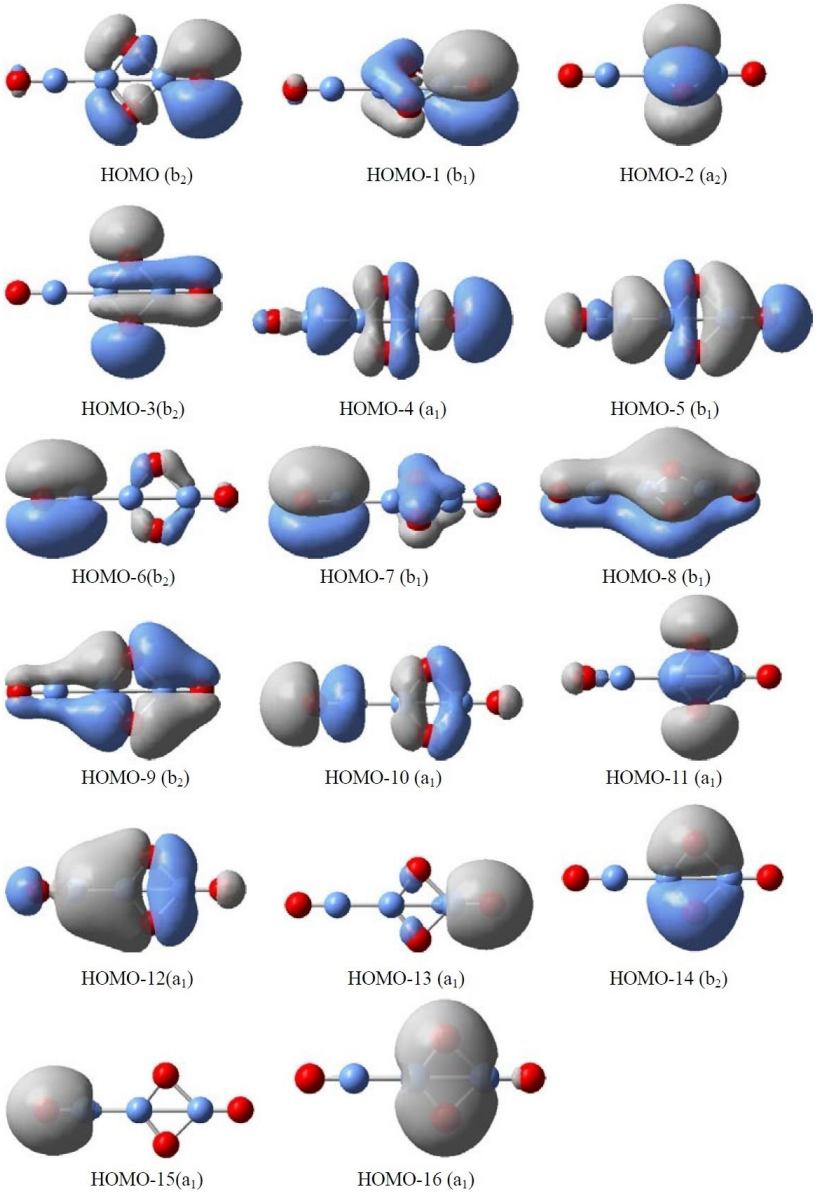

Figure S14. (a) AdNDP bonding pattern for the C_s B_3O_4 (**8**, $^2A'$) global-minimum structure and (b) its canonical molecular orbitals (CMOs).

(a)

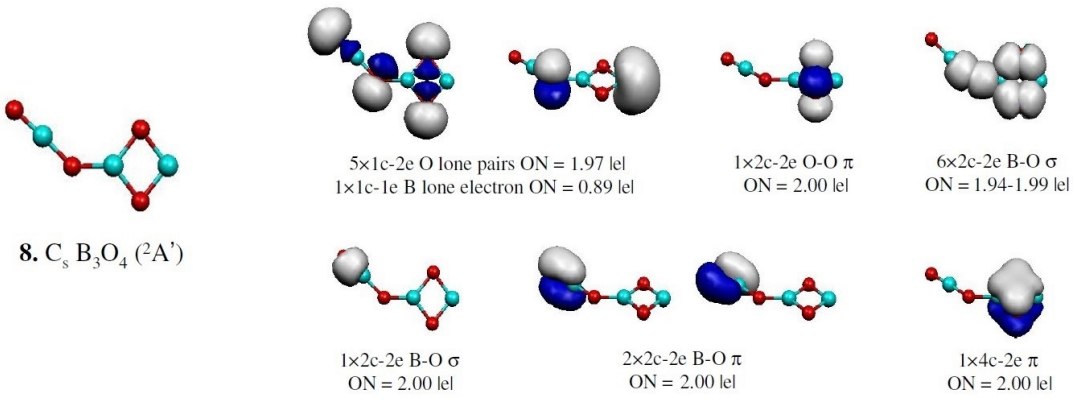

(b)

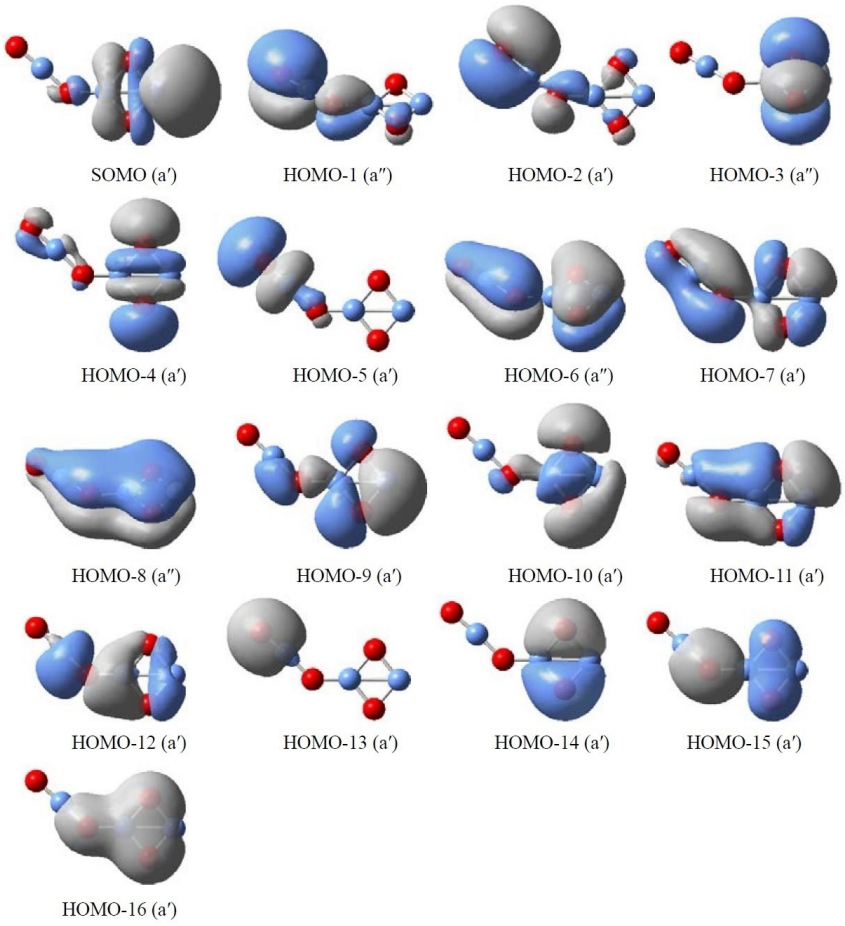

Figure S15. (a) AdNDP bonding pattern for the $D_{\infty h}$ $B_3O_4^+$ (**9**, $^1\Sigma_g$) global-minimum structure and (b) its canonical molecular orbitals (CMOs).

(a)

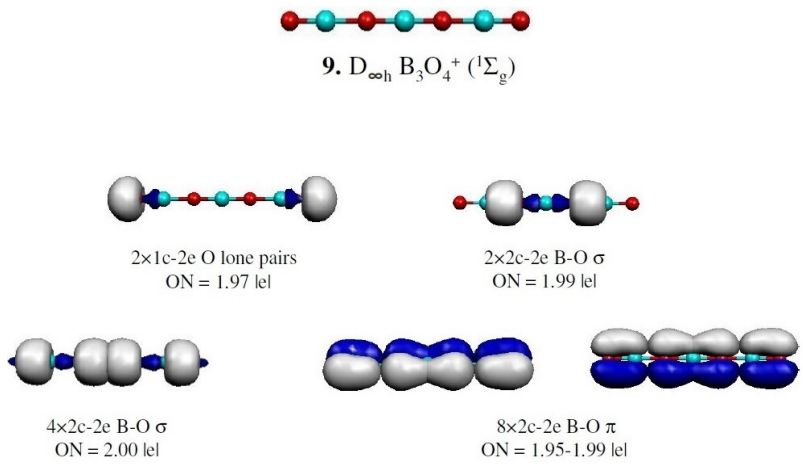

(b)